J. Fluid Mech. (1992), *vol.* 244, *pp.* 477–491

A Monte Carlo solution for rapidly shearing granular flows based on the kinetic theory of dense gases

By MARK A. HOPKINS[1] AND HAYLEY H. SHEN[2]

[1] US Army Corps of Engineers Cold Regions Research and Engineering Laboratory, 72 Lyme Road, Hanover, NH 03755, USA

[2] Department of Civil and Environmental Engineering, Clarkson University, Potsdam, NY 13676, USA

(Received 26 April 1991 and in revised form 20 February 1992)

A Monte Carlo simulation is developed for the study of rapidly deforming, steady, simple shear flows of inelastic disks or spheres. The simulation is based on the theoretical framework of the kinetic theory of dense gases. In the simulation, space is discarded in an explicit sense and replaced by an isotropic, homogeneous, and uncorrelated space based on the assumption of a state of simple shear, a uniform concentration field, and molecular chaos. The simulation generates a distribution of particle velocities which corresponds to the parameters of the flow. The velocity distribution is a numerical solution to the Boltzmann equation under these conditions. The Monte Carlo simulation defines the limits to the accuracy of analytical granular flow theories based on the kinetic theory and the assumption of molecular chaos.

1. Introduction

The flow of granular material is an important transport process that occurs in numerous industrial applications and in many geophysical settings. Examples of such granular flows are found in powder technology, in grain handling, in slurry transport by pipeline, in avalanches, and in the transport of sediment and ice in rivers and oceans.

Bagnold (1954) began the study of rapidly shearing granular flows. He argued that because both the collision frequency and the momentum transferred by collisions between grains were proportional to the rate of shear, the stresses must be proportional to the square of the rate of shear. Savage & Jeffrey (1981), building on the work of Chapman & Cowling (1970), placed the problem of rapidly shearing granular flows in the context of the kinetic theory of dense gases.

In the framework of the kinetic theory of dense gases, as a result of a collision between two particles, a quantity ψ, which depends on velocity, changes to ψ^*. The general form of the collisional rate of change of ψ per unit volume $C(\psi)$ in a system of identical spheres was expressed by Jenkins & Savage (1983) as

$$C(\psi) = \iiint (\psi_2^* - \psi_2) f^{(2)}(\boldsymbol{c}_1, \boldsymbol{r}_1, \boldsymbol{c}_2, \boldsymbol{r}_2)\, \sigma^2 [(\boldsymbol{c}_1 - \boldsymbol{c}_2)\cdot \boldsymbol{k}]\, \mathrm{d}\boldsymbol{k}\, \mathrm{d}\boldsymbol{c}_1\, \mathrm{d}\boldsymbol{c}_2, \tag{i}$$

where $\boldsymbol{r}$ and $\boldsymbol{c}$ denote, respectively, the positions and velocities of the two spheres, $\boldsymbol{k}$ is a unit vector on the line connecting the centre of sphere 1 to the centre of sphere

2, and σ is the diameter. The function $f^{(2)}(\boldsymbol{c}_1, \boldsymbol{r}_1, \boldsymbol{c}_2, \boldsymbol{r}_2)$ is the general form of the pair distribution function which defines the likelihood of finding a pair of particles with their centres located at the points $\boldsymbol{r}_1$ and $\boldsymbol{r}_2$ (separated by a distance σ) with velocities $\boldsymbol{c}_1$ and $\boldsymbol{c}_2$.

A simpler form of (i), used by granular flow theories based on the kinetic theory of dense gases, follows from the assumption of molecular chaos. The implications of that assumption are that the positions and velocities of colliding particles are uncorrelated. This assumption allows the pair distribution function $f^{(2)}$ in (i) to be replaced by the product of two independent single particle velocity distributions $f^{(1)}$ and an isotropic radial distribution function χ. The isotropic radial distribution function, which depends on the solid fraction, defines the likelihood of finding two particles in contact. With these simplifications (i) becomes

$$C(\psi) = \chi \iiint (\psi_2^* - \psi_2) f^{(1)}(\boldsymbol{c}_1, \boldsymbol{r}_1) f^{(1)}(\boldsymbol{c}_2, \boldsymbol{r}_1 + \sigma \boldsymbol{k})\, \sigma^2 [(\boldsymbol{c}_1 - \boldsymbol{c}_2) \cdot \boldsymbol{k}]\, \mathrm{d}\boldsymbol{k}\, \mathrm{d}\boldsymbol{c}_1\, \mathrm{d}\boldsymbol{c}_2. \quad \text{(ii)}$$

Subsequent granular flow theories, following Jenkins & Savage (Lun *et al.* 1984; Jenkins & Richman 1988; Richman & Chou 1992), have generated more accurate constitutive relations, in comparison with full Newtonian particle simulations (Campbell 1989; Walton 1983; Walton & Braun 1986), by using more accurate approximations of the single particle velocity distribution.

Jenkins & Richman (1988) derived constitutive relations for a system of identical, smooth disks from the balance equations for the second moment of the particle velocities. The solution was based on the assumption of molecular chaos and a modified Maxwellian form for the velocity distribution. The mathematical form of the solution removed the restriction to nearly elastic particles common to previous solutions. However, the constitutive relations had separate forms in the dilute and dense limits. Recently, using the same approach, Richman & Chou (1992) derived constitutive relations for a system of identical, smooth spheres valid for all solid fractions.

The subject of the present work is the development of a Monte Carlo simulation of a rapidly deforming simple shear flow of identical disks or spheres. The single particle velocity distribution $f^{(1)}$ is created by the simulation, in accordance with the given flow parameters (shear rate, solid fraction, particle size, and material parameters) and the assumption of molecular chaos. Given the velocity distribution, the analytical equations for the stresses, the energy dissipation, and other measures of the flow may be numerically integrated.

2. Definitions and governing equations

An idealized granular system composed of identical spheres in a steady, simple shear flow is considered. A Cartesian reference frame is used in which the x-axis is aligned with the mean velocity and the y-axis is aligned with the gradient of the mean velocity. The diameter of the spheres is σ and their material properties are characterized by a density ρ, a friction coefficient μ, and a coefficient of restitution e. The velocity of a sphere located at $\boldsymbol{r}$ in the volume element $\mathrm{d}\boldsymbol{r}$ in the flow domain is $\boldsymbol{c}(\boldsymbol{r})$. This velocity has a mean component defined in terms of a constant velocity gradient $\nabla u = \mathrm{d}u/\mathrm{d}y$ by the equation

$$\boldsymbol{u}(\boldsymbol{r}) = \boldsymbol{r} \cdot \nabla \boldsymbol{u}, \quad (1)$$

and a fluctuating component $\boldsymbol{C}(\boldsymbol{r})$ relative to the mean velocity. The relationship among the velocity components is

$$\boldsymbol{c}(\boldsymbol{r}) = \boldsymbol{u}(\boldsymbol{r}) + \boldsymbol{C}(\boldsymbol{r}). \tag{2}$$

The sphere number density, which is assumed to be constant over the region of simple shear, is n. The probable number of sphere centres at $\boldsymbol{r}$ in the volume element $\mathrm{d}\boldsymbol{r}$ about $\boldsymbol{r}$ is $n\,\mathrm{d}\boldsymbol{r}$. A single particle velocity distribution $f^{(1)}(\boldsymbol{c},\boldsymbol{r})$ is defined such that $nf^{(1)}(\boldsymbol{c},\boldsymbol{r})\,\mathrm{d}\boldsymbol{c}\,\mathrm{d}\boldsymbol{r}$ is the probable number of spheres with centres at $\boldsymbol{r}$ in $\mathrm{d}\boldsymbol{r}$ and with velocity $\boldsymbol{c}$ in $\mathrm{d}\boldsymbol{c}$ at any given time. The integral of $f^{(1)}(\boldsymbol{c},\boldsymbol{r})$ over the velocity space is

$$\int f^{(1)}(\boldsymbol{c},\boldsymbol{r})\,\mathrm{d}\boldsymbol{c} = 1. \tag{3}$$

Because the mean velocity gradient is constant, the distribution of fluctuating velocities $f^{(1)}(\boldsymbol{C})$ is independent of position in the shear field. It is related to the single particle velocity distribution $f^{(1)}(\boldsymbol{c},\boldsymbol{r})$:

$$f^{(1)}[\boldsymbol{C}(\boldsymbol{r})] = f^{(1)}[\boldsymbol{c}(\boldsymbol{r}) - \boldsymbol{u}(\boldsymbol{r}), \boldsymbol{r}]. \tag{4}$$

The Boltzmann equation describing the evolution of the fluctuating velocity distribution $f^{(1)}(\boldsymbol{C})$, derived by Chapman & Cowling (1970), is

$$\frac{\partial f}{\partial t} - \frac{\partial \boldsymbol{u}}{\partial t}\cdot\frac{\partial f}{\partial \boldsymbol{C}} + (\boldsymbol{u}+\boldsymbol{C})\cdot\left(\frac{\partial f}{\partial \boldsymbol{r}} - \boldsymbol{\nabla u}\cdot\frac{\partial f}{\partial \boldsymbol{C}}\right) + \boldsymbol{F}\frac{\partial f}{\partial \boldsymbol{C}} = \left(\frac{\partial f}{\partial t}\right)_{\mathrm{c}}, \tag{5}$$

where $\boldsymbol{F}(t,\boldsymbol{r})$ is an external force and $(\partial/\partial t)_{\mathrm{c}}$ denotes rate of change due to collisions. In a steady, simple shear flow, $\partial/\partial t = 0$, $\boldsymbol{u}\cdot\boldsymbol{\nabla u} = 0$, and $\boldsymbol{F} = 0$. The assumptions of simple shear flow and a uniform concentration field imply that $\partial f/\partial r = 0$. The resulting simplified form of the Boltzmann equation expressed in terms of the fluctuating velocity distribution is

$$-\boldsymbol{C}\cdot\boldsymbol{\nabla u}\cdot\frac{\partial f}{\partial \boldsymbol{C}} = \left(\frac{\partial f}{\partial t}\right)_{\mathrm{c}}. \tag{6}$$

Equation (6) states that in steady, simple shear flow, the rate of change of the fluctuating velocity distribution $f^{(1)}(\boldsymbol{C})$ owing to particle motion with respect to the mean velocity field (the left-hand side) is balanced by the rate of change of $f^{(1)}(\boldsymbol{C})$ owing to collisions (the right-hand side).

Conservation of mass is trivially satisfied, since the particles are assumed to be distributed uniformly in space. The balance equations for the conservation of momentum and kinetic energy in a steady, simple shear flow (Jenkins & Savage 1983) reduce to

$$\boldsymbol{P}^{\mathrm{k}} + \boldsymbol{P}^{\mathrm{c}} = \text{constant}, \tag{7}$$

$$\boldsymbol{\nabla u}:(\boldsymbol{P}^{\mathrm{k}} + \boldsymbol{P}^{\mathrm{c}}) = \gamma, \tag{8}$$

where $\boldsymbol{P}^{\mathrm{k}}$ and $\boldsymbol{P}^{\mathrm{c}}$ are, respectively, the kinetic and the collisional components of the stress tensor and γ is the rate of collisional dissipation of fluctuating kinetic energy.

3. Derivation of the distribution of collisional configurations

A more detailed discussion of the following rather brief derivation of the frequency of collisional integral from the kinetic theory of dense gases may be found in Chapman & Cowling (1970). Collisions among the spheres are assumed to be binary and impulsive, that is to say, instantaneous.

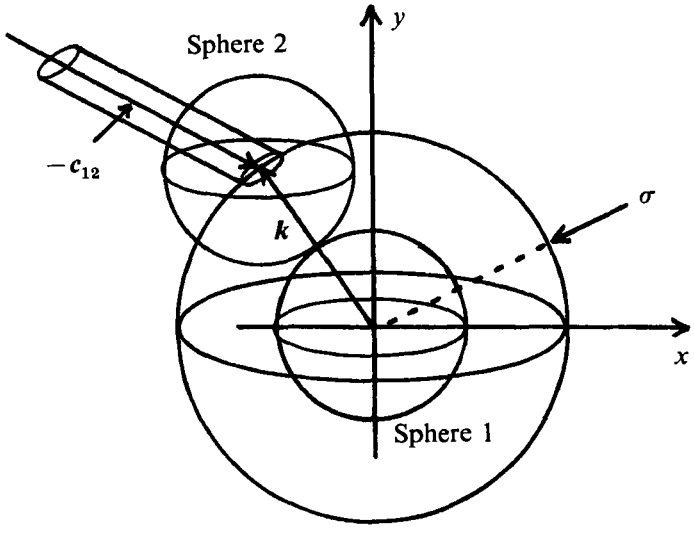

FIGURE 1. A pair of identical spheres in contact.

A pair of identical spheres in contact is shown in figure 1. The vector from the centre of sphere 1 to the centre of sphere 2 is $\sigma\boldsymbol{k} = \boldsymbol{r}_2 - \boldsymbol{r}_1$. The relative velocity of sphere 1 with respect to sphere 2 is $\boldsymbol{c}_{12} = \boldsymbol{c}_1 - \boldsymbol{c}_2$. A collision will occur between two spheres in contact if $\boldsymbol{c}_{12}\cdot\boldsymbol{k} > 0$. In the time interval Δt, prior to a collision, the centre of sphere 2 must be located within the cylinder about $\boldsymbol{c}_{12}$ shown in figure 1. The base of the cylinder is the area $\sigma^2\,\mathrm{d}\boldsymbol{k}$ described by the solid angle $\mathrm{d}\boldsymbol{k}$ about $\boldsymbol{k}$ on the associated sphere of radius σ about sphere 1. The volume of the cylinder is $\sigma^2(\boldsymbol{c}_{12}\cdot\boldsymbol{k})\,\mathrm{d}\boldsymbol{k}\,\Delta t$. As Δt approaches $\mathrm{d}t$ it becomes an infinitesimally thin disk on the associated sphere. The number density at the surface of the associated sphere is $n\chi$ where $\chi(\nu)$, a function of the solid fraction ν, is the limiting value of the isotropic radial distribution function $\chi(\boldsymbol{r},\nu)$ at $r = \sigma$. An analytic expression for $\chi(\nu)$ determined numerically by Carnahan & Starling (1969) for a system of identical spheres is

$$\chi(\nu) = \tfrac{1}{2}(2-\nu)/(1-\nu)^3. \tag{9}$$

The probable number of spheres with centres in the infinitesimal disk on the associated sphere about sphere 1 at a point defined by $\boldsymbol{k}$ with velocity $\boldsymbol{c}_2$ in $\mathrm{d}\boldsymbol{c}_2$ at any given time is

$$n\chi f^{(1)}(\boldsymbol{c}_2, \boldsymbol{r}_1 + \sigma\boldsymbol{k})\,\sigma^2(\boldsymbol{c}_{12}\cdot\boldsymbol{k})\,\mathrm{d}\boldsymbol{k}\,\mathrm{d}\boldsymbol{c}_2\,\mathrm{d}t.$$

A specific collisional configuration in which the centre of sphere 2 is located at $\sigma\boldsymbol{k}$ with respect to the centre of sphere 1 with the velocity $\boldsymbol{c}_2$ in $\mathrm{d}\boldsymbol{c}_2$ and sphere 1 has the velocity $\boldsymbol{c}_1$ in $\mathrm{d}\boldsymbol{c}_1$ is denoted by the triad of vectors $(\boldsymbol{c}_1, \boldsymbol{c}_2, \boldsymbol{k})$. The probable number of such collisional configurations which occur per unit volume per unit time is

$$n^2\chi f^{(1)}(\boldsymbol{c}_1, \boldsymbol{r}_1) f^{(1)}(\boldsymbol{c}_2, \boldsymbol{r}_1 + \sigma\boldsymbol{k})\,\sigma^2(\boldsymbol{c}_{12}\cdot\boldsymbol{k})\,\mathrm{d}\boldsymbol{k}\,\mathrm{d}\boldsymbol{c}_1\,\mathrm{d}\boldsymbol{c}_2. \tag{10}$$

The frequency of collision per unit volume N_{12} is the integral of (10) over all collisional configurations where $\boldsymbol{c}_{12}\cdot\boldsymbol{k} > 0$:

$$N_{12} = \tfrac{1}{2}n^2\chi \iiint f^{(1)}(\boldsymbol{c}_1, \boldsymbol{r}_1) f^{(1)}(\boldsymbol{c}_2, \boldsymbol{r}_1 + \sigma\boldsymbol{k})\,\sigma^2(\boldsymbol{c}_{12}\cdot\boldsymbol{k})\,\mathrm{d}\boldsymbol{k}\,\mathrm{d}\boldsymbol{c}_1\,\mathrm{d}\boldsymbol{c}_2. \tag{11}$$

The independence of the single particle velocity distributions follows from the assumption of molecular chaos.

The normalized distribution of collisional configurations $C^{(2)}(\boldsymbol{c}_1, \boldsymbol{c}_2, \boldsymbol{k})$ which follows from (10) is

$$C^{(2)}(\boldsymbol{c}_1, \boldsymbol{c}_2, \boldsymbol{k}) = \frac{f^{(1)}(\boldsymbol{c}_1, \boldsymbol{r}_1) f^{(1)}(\boldsymbol{c}_2, \boldsymbol{r}_1 + \sigma\boldsymbol{k}) (\boldsymbol{c}_{12} \cdot \boldsymbol{k})}{\iiint f^{(1)}(\boldsymbol{c}_1, \boldsymbol{r}_1) f^{(1)}(\boldsymbol{c}_2, \boldsymbol{r}_1 + \sigma\boldsymbol{k}) (\boldsymbol{c}_{12} \cdot \boldsymbol{k}) \, \mathrm{d}\boldsymbol{k} \, \mathrm{d}\boldsymbol{c}_1 \, \mathrm{d}\boldsymbol{c}_2}. \tag{12}$$

Within the limitations of the assumption of molecular chaos, $C^{(2)}$ represents the distribution of collisional configurations, or colliding pairs of particles, which would be found in a real system with the same physical parameters (shear rate, solid fraction, sphere diameter, and material properties). That is, $C^{(2)}(\boldsymbol{c}_1, \boldsymbol{c}_2, \boldsymbol{k}) \, \mathrm{d}\boldsymbol{k} \, \mathrm{d}\boldsymbol{c}_1 \, \mathrm{d}\boldsymbol{c}_2$ is the fraction of collisional configurations with $\boldsymbol{c}_1$ in $\mathrm{d}\boldsymbol{c}_1$, $\boldsymbol{c}_2$ in $\mathrm{d}\boldsymbol{c}_2$, and $\boldsymbol{k}$ in $\mathrm{d}\boldsymbol{k}$ in the set of all collisional configurations. In contrast, the distribution $F^{(2)}(\boldsymbol{c}_1, \boldsymbol{c}_2, \boldsymbol{k})$ where

$$F^{(2)}(\boldsymbol{c}_1, \boldsymbol{c}_2, \boldsymbol{k}) = f^{(1)}(\boldsymbol{c}_1, \boldsymbol{r}_1) f^{(1)}(\boldsymbol{c}_2, \boldsymbol{r}_1 + \sigma\boldsymbol{k}) \left(\int \mathrm{d}\boldsymbol{k} \right)^{-1} \tag{13}$$

defines the distribution of configurations with $\boldsymbol{c}_1$ and $\boldsymbol{c}_2$ and $\boldsymbol{k}$ chosen at random.

In the Monte Carlo simulation a collisional configuration is constructed by choosing a pair of particle velocities $\boldsymbol{c}_1$ and $\boldsymbol{c}_2$ randomly from the single particle velocity distribution $f^{(1)}$ represented by an array in the computer memory and by specifying the position of particle 2 with respect to particle 1 by randomly choosing a direction $\boldsymbol{k}$. The distribution of the configurations so chosen is defined by $F^{(2)}$. A subset of configurations is chosen, from the set of configurations chosen at random defined by $F^{(2)}$, in such a manner that the distribution of configurations in the subset is defined by $C^{(2)}$. The post-collision velocities which result from the collisions occurring in the subset $C^{(2)}$ of collisional configurations replace the pre-collision velocities chosen from the array which represents the single particle velocity distribution $f^{(1)}$.

4. The Monte Carlo simulation

A single particle velocity distribution $f^{(1)}$ may be approximately determined by recording the velocities of particles passing through a small window in a real system over a sufficient period of time. Similarly, $f^{(1)}$ is defined in the Monte Carlo simulation by the flow of particle velocities through a velocity array defined in the computer memory over the course of the simulation. In a statistical sense, the current state of the velocity array in the Monte Carlo simulation is analogous to the current velocities of a like number of particles in the real system.

The first step in the Monte Carlo simulation is the definition of an array to represent $f^{(1)}(\boldsymbol{C})$, the distribution of fluctuating velocities. The array is dimensioned to contain the translational and rotational components of n velocities. This array may be thought of as containing the current fluctuating velocities of n spheres in the system being simulated. If the array were sampled over a sufficiently long interval, the sample would approximate the velocity distribution $f^{(1)}$. The velocities in the array are initialized to zero.

A collisional configuration $(\boldsymbol{c}_1, \boldsymbol{c}_2, \boldsymbol{k})$ is created by choosing the fluctuating velocities $\boldsymbol{C}_1$ and $\boldsymbol{C}_2$ at random from the array and a direction $\boldsymbol{k}$ uniformly at random in space. The particle velocities $\boldsymbol{c}_1$ and $\boldsymbol{c}_2$ relative to the mean velocity at the point

of contact, are constructed by adding a mean velocity component to the chosen fluctuating velocities $\boldsymbol{C}_1$ and $\boldsymbol{C}_2$:

$$\boldsymbol{c}_1 = \boldsymbol{C}_1 - \tfrac{1}{2}\sigma \boldsymbol{k}\cdot\nabla\boldsymbol{u}, \tag{14a}$$

$$\boldsymbol{c}_2 = \boldsymbol{C}_2 + \tfrac{1}{2}\sigma \boldsymbol{k}\cdot\nabla\boldsymbol{u}. \tag{14b}$$

The configurations chosen at random belong to the set of configurations defined by the distribution $F^{(2)}$ (equation (13)). In order to create the subset of configurations defined by the distribution $C^{(2)}$ (equation (12)), the constraint

$$\boldsymbol{c}_{12}\cdot\boldsymbol{k} - \beta R > 0 \tag{15}$$

is imposed on each configuration in the set chosen at random. In (15), R is a number chosen anew with each configuration from a random sequence distributed uniformly between 0 and 1, and β is a constant parameter, greater than any value of $\boldsymbol{c}_{12}\cdot\boldsymbol{k}$ which is likely to be encountered during the simulation. The configurations which satisfy this constraint belong to the subset of configurations defined by $C^{(2)}$.

$F^{(2)}(\boldsymbol{c}_1, \boldsymbol{c}_2, \boldsymbol{k})\,\mathrm{d}\boldsymbol{k}\,\mathrm{d}\boldsymbol{c}_1\,\mathrm{d}\boldsymbol{c}_2$ is the fraction of configurations chosen at random with $\boldsymbol{c}_1$ in $\mathrm{d}\boldsymbol{c}_1$, $\boldsymbol{c}_2$, in $\mathrm{d}\boldsymbol{c}_2$ and $\boldsymbol{k}$ in $\mathrm{d}\boldsymbol{k}$. The fraction of these configurations which satisfy the constraint (15) is $(\boldsymbol{c}_{12}\cdot\boldsymbol{k})/\beta$. Therefore the effect of applying the constraint to the configurations chosen at random is to multiply the distribution of configurations chosen at random $F^{(2)}$ by $(\boldsymbol{c}_{12}\cdot\boldsymbol{k})/\beta$. This produces the distribution of collisional configurations $C^{(2)}$ scaled by $\langle \boldsymbol{c}_{12}\cdot\boldsymbol{k}\rangle/\beta$, where $\langle\ \rangle$ denotes expected value. Although the distribution $C^{(2)}$ is scaled, the probability of one collisional configuration $(\boldsymbol{c}_1, \boldsymbol{c}_2, \boldsymbol{k})$ occurring relative to any other is preserved.

Collisions are generated from the set of randomly chosen collisional configurations. The post-collision velocities are calculated from a given configuration $(\boldsymbol{c}_1, \boldsymbol{c}_2, \boldsymbol{k})$ using a rigid particle collision model derived from the balance laws for linear and angular momentum conservation and closure conditions for friction and restitution. The collision model is described in the Appendix.

In a real system, a particle's pre-collision velocity is replaced by its post-collision velocity. In the Monte Carlo simulation the velocity state of the system is represented by the n-dimensioned velocity array. Therefore, in the collisions which occur in the subset of configurations $C^{(2)}$ which satisfy the constraint (15), the pre-collision velocities of the spheres are replaced in the array by the corresponding post-collision velocities. The pre-collision velocities $\boldsymbol{C}_1$ and $\boldsymbol{C}_2$ are replaced by the fluctuating components of the post-collision velocities $\boldsymbol{c}_1^*$ and $\boldsymbol{c}_2^*$:

$$\boldsymbol{C}_1^* = \boldsymbol{c}_1^* + \tfrac{1}{2}\sigma\boldsymbol{k}\cdot\nabla\boldsymbol{u}, \quad \boldsymbol{C}_2^* = \boldsymbol{c}_2^* - \tfrac{1}{2}\sigma\boldsymbol{k}\cdot\nabla\boldsymbol{u}. \tag{16a, b}$$

Again, in a real system, as a particle moves through the shear field in the direction of the mean velocity gradient, its absolute velocity remains constant, while the mean velocity measured at the location of the particle's centre changes. Therefore, its fluctuating velocity, which is the difference between the two, changes also. The rate of change of fluctuating velocity owing to translation is

$$\mathrm{d}\boldsymbol{C}/\mathrm{d}t = -\boldsymbol{C}\cdot\nabla\boldsymbol{u}, \tag{17a}$$

which may be expressed in finite difference form as

$$\boldsymbol{C}_i^{n+1} = \boldsymbol{C}_i^n - \boldsymbol{C}_i^n\cdot\nabla\boldsymbol{u}\,\Delta t, \tag{17b}$$

where the superscript n denotes time and the subscript i denotes a particle. The change in fluctuating velocity owing to translation is modelled in the Monte Carlo simulation by applying (17b) to the translational component of each velocity $\boldsymbol{C}_i$ in

the velocity array after each collision which satisfies the constraint (15). The timestep Δt in (17*b*) is the reciprocal of the average frequency of collision N_{12} which is calculated using the numerical equivalent of (11)

$$N_{12} = \pi n^2 \chi \sigma^2 \langle \boldsymbol{c}_{12} \cdot \boldsymbol{k} \rangle, \tag{18}$$

where $\langle\ \rangle$ denotes an average over each collision in the set of configurations chosen at random.

In summary, a step in the simulation process consists of choosing a configuration at random and calculating post-collision velocities. If the configuration satisfies the constraint (15), then the two pre-collision velocities chosen from the array are replaced by the post-collision velocities, and the rest of the fluctuating velocities in the array are updated by applying (17*b*). The timestep Δt in (17*b*) is the reciprocal of the average frequency of collision (18) which is calculated concurrently in the simulation over a period of a large number of collisions in an iterative fashion. To begin the simulation, an initial frequency of collision is assumed. After a large number of collisions, the frequency of collision is recalculated and the simulation continues. As this iterative process is repeated, the frequency of collision approaches a stationary value. At the same time, the velocity distribution $f^{(1)}$, obtained by sampling the entire velocity array uniformly at regular intervals, becomes statistically stationary.

It is essential to emphasize the difference between the collisions in the set of configurations chosen at random (described by $F^{(2)}$) and the subset of these configurations (described by $C^{(2)}$) which satisfy the constraint (15). The collisions in the subset of configurations which satisfy (15) are used to create the velocity distribution $f^{(1)}$ by replacing the pre-collision velocities chosen from the array by post-collision velocities. Given the velocity distribution $f^{(1)}$ it is then possible to numerically integrate the theoretical expressions for the frequency of collision (18) and the stresses, which are discussed below. In the integration of the frequency of collision and the stresses, all of the collisions in the set of configurations chosen at random are used.

5. The solution of the Boltzmann equation

Equation (17*a*) is similar to the left-hand side of (6), the Boltzmann equation for a steady, simple shear flow. Equation (17*b*) is applied to each velocity in the array at each timestep during the Monte Carlo simulation. Since the array represents the velocity distribution $f^{(1)}$, (17*b*) is, in effect, applied to the velocity distribution at each timestep. The changes depend on $\boldsymbol{C}$. Taking the dot product of (17*a*) with $\partial f/\partial \boldsymbol{C}$ yields

$$\frac{\partial \boldsymbol{C}}{\partial t} \cdot \frac{\partial f}{\partial \boldsymbol{C}} = \frac{\partial f}{\partial t} = -\boldsymbol{C} \cdot \nabla \boldsymbol{u} \cdot \frac{\partial f}{\partial \boldsymbol{C}}. \tag{19}$$

This equation describes the change in f owing to convection, which is the left-hand side of (6), the simplified Boltzmann equation. Equation (6) states that in steady, simple shear flow, the rate of change of the fluctuating velocity distribution $f^{(1)}(\boldsymbol{C})$ owing to particle motion with respect to the mean velocity field is balanced by the rate of change of $f^{(1)}(\boldsymbol{C})$ owing to collisions. This is precisely what occurs in the Monte Carlo simulation where changes to the velocity array by collisions are balanced, at steady state, by the changes to the velocity array resulting from the use of (17*b*). A corollary to this argument is that the energy dissipated in collisions is resupplied from the mean shear flow.

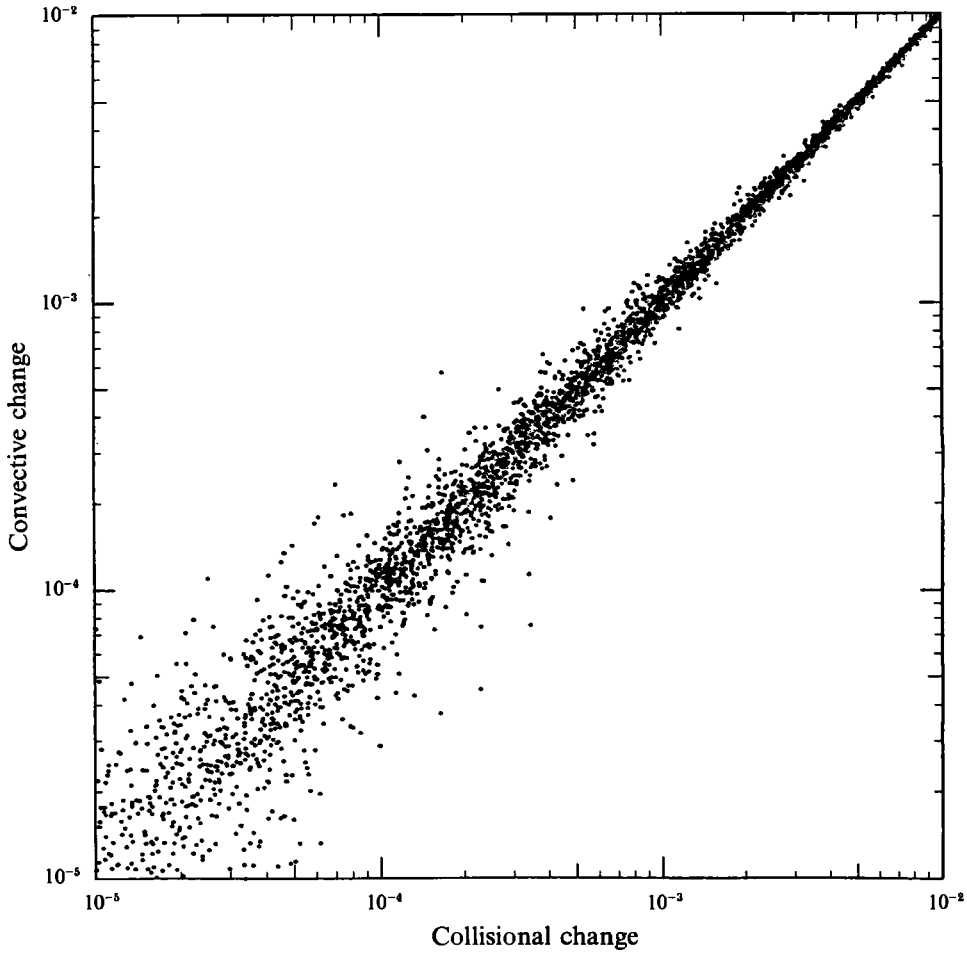

FIGURE 2. The solution of (20), the finite-difference form of (6), the simplified Boltzmann equation for a steady, simple shear flow of identical spheres with $\nu = 0.3$, $e = 0.3$, $\mu = 0$, $n = 200$, and $\mathrm{d}u/\mathrm{d}y = 1$.

In order to demonstrate more clearly that the velocity distribution generated by the Monte Carlo simulation is a solution to the simplified Boltzmann equation, we compare the two sides of (6) using the generated velocity distribution.

The Monte Carlo simulation was run for 20 million collisions for $\nu = 0.3$, $e = 0.3$, $\mu = 0$, $n = 200$, and $\mathrm{d}u/\mathrm{d}y = 1$. During the simulation, three distinct velocity distributions were compiled. The three distributions were constructed by sorting the x-, y-, and z-components of velocities into three-dimensional $(86 \times 70 \times 70)$ arrays. The dimensions of the arrays allowed ranges of about 3.5 standard deviations of each velocity component in both the positive and negative directions. The first array was $f^{(1)}(\boldsymbol{C})$, the distribution of velocities found in the flow. This was constructed by sorting the entire n-dimension velocity array discussed above into the distribution array at intervals of n collisions. The second array was an array of pre-collision velocities. This was constructed by sorting each pair of pre-collision velocities into the array prior to each collision satisfying constraint (15). The third array was an array of post-collision velocities. This was constructed by sorting each pair of post-collision velocities into the array following each collision satisfying constraint (15).

The arrays were normalized following the simulation to yield probability density functions defining the general distribution of particle velocities $f^{(1)}$, the distribution of pre-collision velocities $f^{(2)}$, and the distribution of post-collision velocities $f^{(3)}$, respectively. Each distribution was zero-padded and smoothed in the x-direction using a low-pass filter with a transition frequency of 0.05 cycle per data interval.

Since a given pre-collision velocity $\boldsymbol{C}$ is destroyed in a collision, the product of the average frequency of collision (equation (18)) and the second distribution is the average rate of destruction of the given velocity. Similarly, the product of the average frequency of collision (equation (18)) and the third distribution is the average rate of creation of a given velocity. The difference between the two represents the net rate of change of $f^{(1)}(\boldsymbol{C})$ owing to collision.

Equation (6) may be rewritten in terms of the three velocity distributions as

$$-C^j \,\mathrm{d}u/\mathrm{d}y\, n[f^{(1)}(C^{i+1,jk})-f^{(1)}(C^{i-1,jk})]/(2\Delta C) = N_{12}[f^{(3)}(C^{ijk})-f^{(2)}(C^{ijk})], \quad (20)$$

where the superscripts i, j, k denote array elements corresponding to the x-, y-, z-components of the chosen velocity. This equation was solved for 10000 randomly chosen values of $\boldsymbol{C}$. For each value of $\boldsymbol{C}$ a circle is plotted on figure 2. The abscissa of the circle corresponds to the value of the left-hand side of (20) and the ordinate corresponds to the value of the right-hand side of (20). The increased scatter at lower values is caused by the decreasing magnitude of the terms relative to the error in the distributions owing to sample size.

6. Stress calculations

Stresses generated in a granular flow have a kinetic component caused by momentum carried across a surface in the flow by particle motion and a collisional stress component caused by momentum transferred across a surface in the flow between colliding particles. The kinetic component of stress $\boldsymbol{P}^{\mathrm{k}}$ is given by the equation

$$\boldsymbol{P}^{\mathrm{k}} = \rho\nu \int f^{(1)}(\boldsymbol{C})\, \boldsymbol{C}\boldsymbol{C}\, \mathrm{d}\boldsymbol{C}. \quad (21)$$

The collisional component of stress $\boldsymbol{P}^{\mathrm{c}}$ is found by averaging the flux of linear momentum $\sigma \boldsymbol{k}\boldsymbol{m}(\boldsymbol{c}_2^* - \boldsymbol{c}_2)$ in a given collisional configuration over all possible configurations occurring per unit volume and time given by (10) in which $\boldsymbol{c}_{12}\cdot\boldsymbol{k} > 0$ as

$$\boldsymbol{P}^{\mathrm{c}} = \tfrac{1}{2} n^2 \chi \iiint f^{(1)}(\boldsymbol{c}_1, \boldsymbol{r}_1) f^{(1)}(\boldsymbol{c}_2, \boldsymbol{r}_1 + \sigma\boldsymbol{k})\, \sigma^2 \boldsymbol{k}\boldsymbol{m}(\boldsymbol{c}_2^* - \boldsymbol{c}_2)\, \sigma(\boldsymbol{c}_{12}\cdot\boldsymbol{k})\, \mathrm{d}\boldsymbol{k}\, \mathrm{d}\boldsymbol{c}_1\, \mathrm{d}\boldsymbol{c}_2. \quad (22)$$

After the velocity array becomes statistically stationary, the analytic expressions for the stresses may be calculated numerically. The expression for the kinetic stress (21) has the numerical equivalent

$$\boldsymbol{P}^{\mathrm{k}} = \rho\nu\langle \boldsymbol{C}\boldsymbol{C}\rangle, \quad (23)$$

where $\langle\ \rangle$ denotes an average over each velocity in the velocity array sampled at uniform time intervals after the array reaches statistical equilibrium. The expression for the collisional stress (22) has the numerical equivalent

$$\boldsymbol{P}^{\mathrm{c}} = \pi n^2 \chi \sigma^3 \langle \boldsymbol{k}\boldsymbol{m}(\boldsymbol{c}_2^* - \boldsymbol{c}_2)\, (\boldsymbol{c}_{12}\cdot\boldsymbol{k})\rangle, \quad (24)$$

where $\langle\ \rangle$ denotes an average over each collision in the set of configurations chosen at random after the velocity array reaches statistical equilibrium.

7. Sensitivity of the Monte Carlo simulation

The size of the velocity array, the period of iteration in the calculation of the frequency of collision, and the parameter β in constraint (15) must be chosen with care. The following suggestions are based on sensitivity studies described in Hopkins (1987). The velocity array should be dimensioned to contain the velocities of at least 100 (imaginary) particles. A greater number of velocities will marginally increase the accuracy, while increasing the running time. Fewer particles may create the random fluctuations characteristic of small systems. At least 100 collisions per particle should be allowed to equilibrate the velocity array. The period between successive calculations of the frequency of collision should be at least 10 collisions per particle. In both cases only those collisions which satisfy (15) are counted.

The value of β used in the constraint (15) should be equal to the largest value of $\boldsymbol{c}_{12}\cdot\boldsymbol{k}$ encountered in the simulation. As long as the chosen value of β is greater than or equal to any value of $\boldsymbol{c}_{12}\cdot\boldsymbol{k}$ encountered during the simulation, the results will be completely insensitive to the value of β. However, if β is made arbitrarily large, the running time of the simulation will increase proportionately. In practice, a value of β five times the expected value $\langle \boldsymbol{c}_{12}\cdot\boldsymbol{k}\rangle$ is sufficient.

8. Simulation of an equilibrium system of smooth, elastic spheres

A Monte Carlo simulation of a system of identical, smooth, elastic spheres in equilibrium was performed. Analytical solutions exist for such a system (Jeans 1948). The simulated system consisted of 125 particles. The velocities were initially of uniform magnitude with random directions. The velocity distribution obtained by sampling the velocity array over a period of 2000000 collisions after the system reached equilibrium was an isotropic Maxwellian given by

$$f^{(1)}(C) = (2\pi T)^{-\frac{3}{2}} C^2 \exp(-C^2/2T), \tag{25}$$

where $T = \frac{1}{3}\langle \boldsymbol{C}\cdot\boldsymbol{C}\rangle$ is the translational temperature which is fixed by the initial velocities of the spheres. In terms of the translational temperature, the stresses in the system at equilibrium are

$$P^{\mathrm{k}} = 3\nu T^2, \tag{26}$$

$$P^{\mathrm{c}} = 12\nu^2\chi T^2. \tag{27}$$

The stresses calculated by the Monte Carlo simulation were within 0.1 % of the exact values. Jeans (1948) also gives an analytical expression for the velocity-dependent mean free path, the mean length of the path travelled by a particle with velocity C between successive collisions. The Monte Carlo results for a period of 2000000 collisions were essentially identical to the values given by Jeans except for extremes of velocity where samples were sparse (Hopkins 1987). The velocity-dependent mean free path involves the residence time of a given velocity in the velocity array between successive collisions (or in real terms, the time between collisions for a particle moving with a given velocity) and, therefore, depends on the constraint (15).

9. Simulation of a rapidly sheared system of identical, smooth spheres

Since no exact solutions exist for systems of spheres in steady, simple shear, the Monte Carlo simulation must be verified by comparison with results obtained from complete Newtonian computer simulations. Hopkins & Louge (1991) contains a

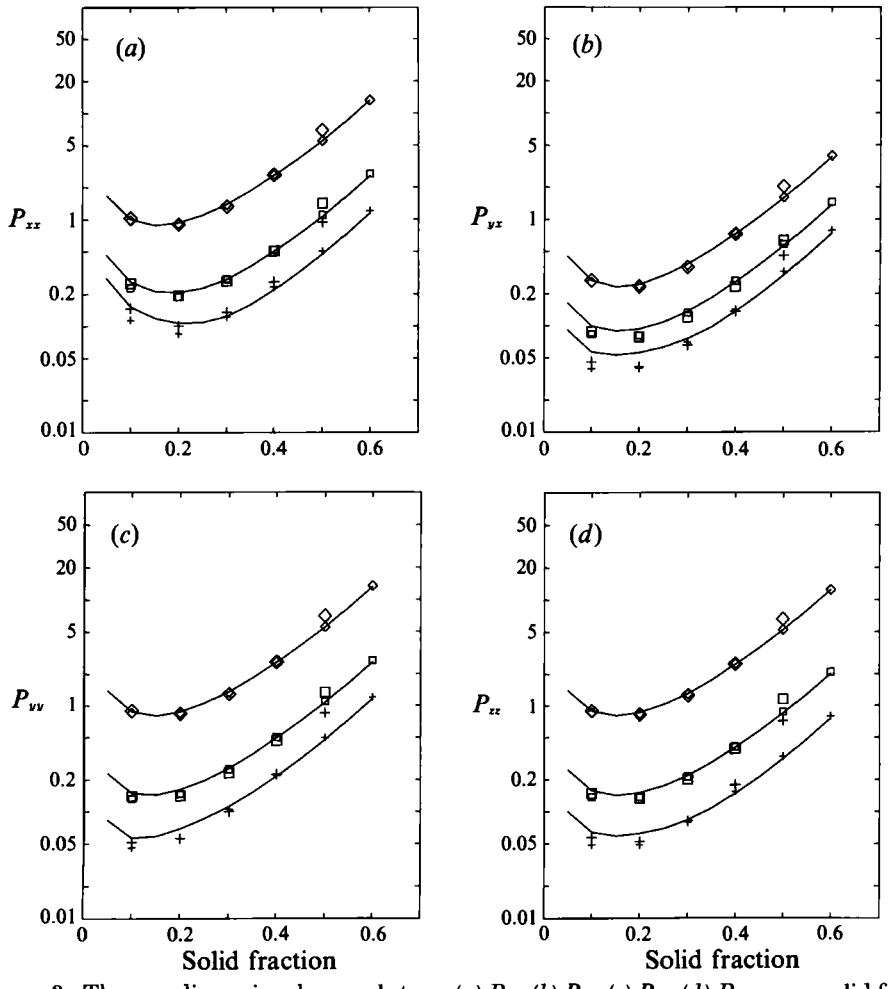

FIGURE 3. The non-dimensional normal stress (*a*) P_{xx}, (*b*) P_{yx}, (*c*) P_{yy}, (*d*) P_{zz} versus solid fraction for a system of uniform diameter, smooth ($\mu = 0$) spheres in simple shear for several values of the coefficient of restitution e, +, $e = 0.3$; □, $e = 0.6$; ◇, $e = 0.9$. ◇, Monte Carlo ; ◇, full simulation; ——, Richman & Chou.

description of the mechanics of a complete simulation of a periodic, steady, simple shear flow. The complete simulation uses the same rigid particle collision model as the Monte Carlo simulation. The collision model is described in the Appendix to the present work.

Richman & Chou (1992) derived constitutive relations for a system of identical, smooth spheres valid for all solid fractions. In figures 3 and 4 the solution of Richman & Chou is compared to the results of the Monte Carlo simulation and the complete Newtonian simulation. Both the full simulations and the Monte Carlo simulations were performed with systems of 125 identical spheres. In both simulations stresses were calculated over a period of 1000 collisions per particle. In the Monte Carlo simulation, the period of iteration for the frequency of collision was 1250 collisions and the parameter β was at least 5 $\langle \boldsymbol{c}_{12} \cdot \boldsymbol{k} \rangle$. In the full simulations, the average overlap between colliding particles (see Hopkins & Louge 1991) was approximately 1% of the calculated mean free path. The figures show the dependence of the stress components P_{xx}, P_{yx}, P_{yy}, and P_{zz} and the ratios P_{yx}/P_{yy}, P_{xx}/P_{yy}, and P_{zz}/P_{yy} on

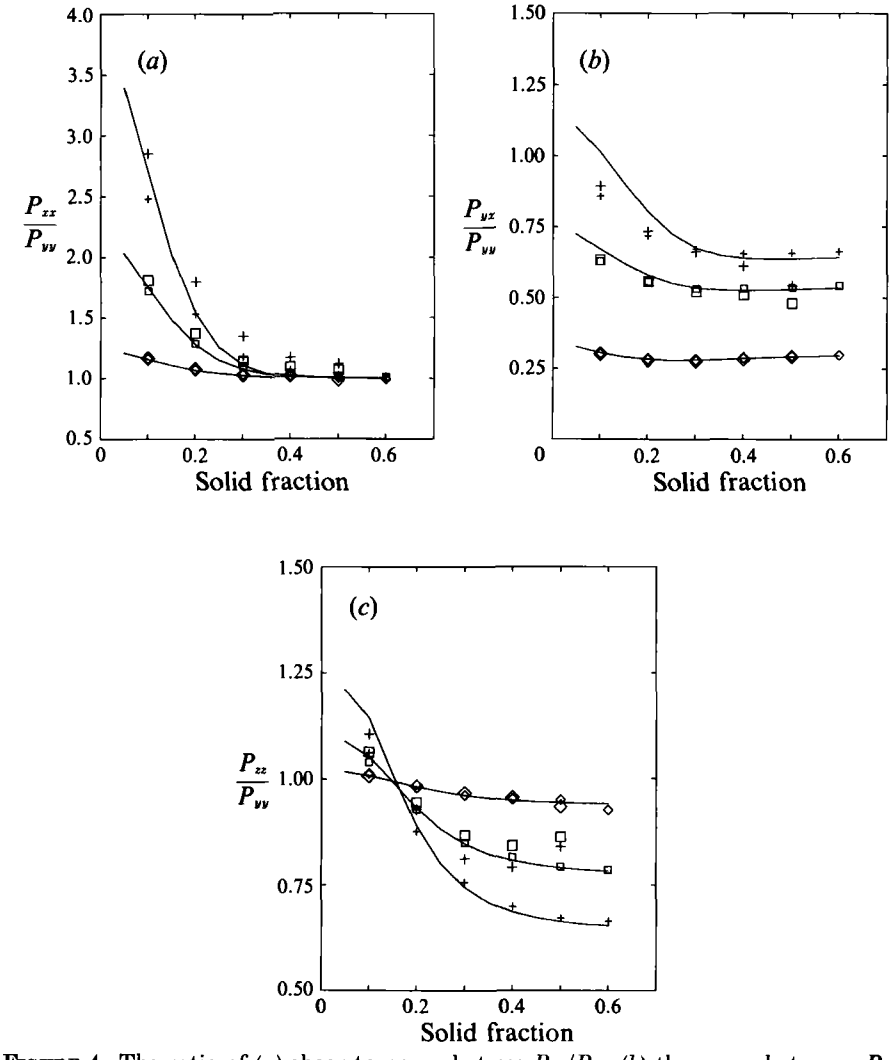

FIGURE 4. The ratio of (*a*) shear to normal stress P_{yx}/P_{yy}, (*b*) the normal stresses P_{xx}/P_{yy}, and (*c*) the normal stresses P_{zz}/P_{yy} versus solid fraction. Key as for figure 3.

the coefficient of restitution e and the solid fraction ν. The stresses are the sum of the kinetic (23) and collisional (24) components and are non-dimensionalized by $\rho(\sigma\,\mathrm{d}u/\mathrm{d}y)^2$. Each figure shows results for three values of e, denoted by crosses, squares, and diamonds. The small symbols, large symbols, and lines denote respectively the results of the Monte Carlo simulation, the full simulation, and the theory of Richmond & Chou. At the highest solid fraction ($\nu = 0.6$), the full simulation was unable to shear the material.

The general agreement of the three data sets is remarkable. However, the results of the Monte Carlo simulation and the complete simulation diverge at low values of the coefficient of restitution and at high solid fractions. The divergence at these extremes is due to the breakdown of the molecular chaos assumption.

10. A general discussion of the results

The breakdown of the molecular chaos assumption implies the emergence of structure or anisotropy and local inhomogeneity in the concentration field. Structure at high densities is expected. Campbell (1986) studied the creation of a distinct, layered microstructure in dense shear flows. Recently Hopkins & Louge (1991) have defined a dynamic microstructure which depends on particle inelasticity. The basic mechanism of the inelastic microstructure is the formation of particle clusters, local regions of above average particle density. Hopkins & Louge report the results of a series of simple shear simulations with identical smooth disks. These results show that the effects of the inelastic microstructure, especially noticeable in the P_{xx} kinetic stress component, are inversely related to the coefficient of restitution and increase with the number density. The divergence shown in figures 3 and 4 between the Monte Carlo simulation and the complete simulation at low values of the coefficient of restitution is probably the result of the inelastic microstructure. The divergence at higher solid fractions is probably the result of the dense microstructure and velocity correlations between colliding particles.

The results of the Monte Carlo simulation and the theory of Richman & Chou diverge at low values of the coefficient of restitution. Since both assume molecular chaos, the differences are probably due to deviations from the joint Maxwellian form of the velocity distribution used in the Richman & Chou theory. The kinetic stress, the dominant component at low solid fractions, being proportional to the second moments of the velocity, is more closely related to the form of the velocity distribution than the collisional stress. The kinetic stress is negligible at moderate to high solid fractions where the Monte Carlo simulation and the theory of Richman & Chou are in total agreement.

11. Conclusions

In this work a Monte Carlo simulation for the study of rapidly deforming, simple shear flows of identical inelastic disks or spheres has been developed. The Monte Carlo simulation is based on the theoretical framework of the kinetic theory of dense gases. In the Monte Carlo simulation, space is discarded in an explicit sense and replaced by an isotropic, homogeneous, and uncorrelated space based on the assumption of a state of simple shear, a uniform concentration field, and molecular chaos. Although, the examples discussed above, in the development of the Monte Carlo simulation, used smooth, frictionless spheres, the simulation applies with equal accuracy to flows of rough spheres.

The Monte Carlo simulation generates the distribution of fluctuating velocities which corresponds to the parameters of the flow (shear rate, solid fraction, particle size and material properties) and the given assumptions. This velocity distribution is a numerical solution to the simplified Boltzmann equation (6) under these conditions, just as the distribution produced by a full, Newtonian simulation is a solution to (6) without the molecular chaos assumption. The Monte Carlo simulation defines the limits to the accuracy of analytical granular flow theories based on the kinetic theory of dense gases and the assumption of molecular chaos. In comparison with the theory of Richman & Chou, it shows that the most sophisticated theories are close to that limit. In comparison with the complete simulations, it shows that further theoretical progress depends on an understanding of microstructure.

The authors would like to acknowledge the support for this work provided by the

National Science Foundation under grants CTS-9009168 and MSM-8419416 and the United States Army Corps of Engineers Cold Regions Research and Engineering Laboratory under grant DACA89-86-K-0015. They would also like to thank Jim Jenkins, Greg Flato, and Sam Colbeck for their suggestions, which have greatly improved the manuscript.

Appendix: Collision model used in the Monte Carlo simulation

Collisions between disks or spheres are assumed to be binary and impulsive. Spheres (disks) have constant coefficients of restitution e and friction μ. The collision equations are derived for the general case in which the particles have different diameters.

A local $(\boldsymbol{n}, \boldsymbol{t})$-coordinate frame is defined with its origin at the point of contact and the normal axis $\boldsymbol{n}$ in the direction of the vector $\sigma \boldsymbol{k}$ from the centre of sphere (disk) 1 to the centre of sphere (disk) 2 (see figure 1). The tangential axis $\boldsymbol{t}$ is the direction of the component of relative velocity at the contact point $\boldsymbol{c}_{12c}$ which is perpendicular to the $\boldsymbol{n}$-axis:

$$\boldsymbol{t} = [\boldsymbol{c}_{12c} - (\boldsymbol{c}_{12c} \cdot \boldsymbol{n})\boldsymbol{n}] / |\boldsymbol{c}_{12c} - (\boldsymbol{c}_{12c} \cdot \boldsymbol{n})\boldsymbol{n}|. \tag{A 1}$$

The relative velocity at the contact point is

$$\boldsymbol{c}_{12c} = \boldsymbol{c}_1 + \boldsymbol{r}_1 \times \boldsymbol{\omega}_1 - \boldsymbol{c}_2 - \boldsymbol{r}_2 \times \boldsymbol{\omega}_2, \tag{A 2}$$

where $\boldsymbol{r}$ is the vector from the point of contact to the centre of the sphere (disk). The post-collision velocities, denoted by an asterisk, are derived from equations for the conservation of linear and angular momentum. The equation describing the conservation of linear momentum is

$$m_2(\boldsymbol{c}_2^* - \boldsymbol{c}_2) = -m_1(\boldsymbol{c}_1^* - \boldsymbol{c}_1) = \boldsymbol{P}, \tag{A 3}$$

where $\boldsymbol{P}$ is the collisional impulse on particle 2. The equations describing the conservation of angular momentum about the point of contact for each sphere (disk) are

$$I_1 \boldsymbol{\omega}_1^* = I_1 \boldsymbol{\omega}_1 + \boldsymbol{r}_1 \times \boldsymbol{P}, \quad I_2 \boldsymbol{\omega}_2^* = I_2 \boldsymbol{\omega}_2 - \boldsymbol{r}_2 \times \boldsymbol{P}, \tag{A 4a, b}$$

where I is the polar moment of inertia. The coefficient of restitution e characterizing the incomplete restitution of translational velocity in the $\boldsymbol{n}$-direction yields

$$(\boldsymbol{c}_1^* - \boldsymbol{c}_2^*) \cdot \boldsymbol{n} = -e(\boldsymbol{c}_1 - \boldsymbol{c}_2) \cdot \boldsymbol{n}. \tag{A 5}$$

The $\boldsymbol{n}$-component of the collisional impulse follows from (A 3) and (A 5):

$$\boldsymbol{P} \cdot \boldsymbol{n} = (1+e)[(m_1 m_2)/(m_1 + m_2)](\boldsymbol{c}_{12c} \cdot \boldsymbol{n}). \tag{A 6}$$

The last equation required to close the system of equations for the post-collision velocities is a frictional closure equation defining the tangential impulse at the point of contact. The tangential component of the impulse is initially assumed given in terms of the normal impulse by a Mohr–Coulomb relationship:

$$\boldsymbol{P} \cdot \boldsymbol{t} = \mu \boldsymbol{P} \cdot \boldsymbol{n}. \tag{A 7}$$

The tangential impulse acts on each particle at the point of contact to retard the tangential component of the relative velocity at the point of contact $\boldsymbol{c}_{12c}$. In collisions in which the relative velocity at the point of contact has a large normal component and a small tangential component, the use of (A 7) may cause a reversal of the relative tangential velocity, which is not allowed. This is accomplished by limiting

the tangential impulse to the value which completely arrests, but does not reverse, the tangential velocity. In this limiting case, the post-collision tangential velocity at the point of contact is zero:

$$\boldsymbol{c}^*_{12c} \cdot \boldsymbol{t} = 0. \tag{A 8}$$

The tangential impulse which follows from (A 3), (A 4*a*, *b*), and (A 8) is

$$\boldsymbol{P} \cdot \boldsymbol{t} = (\boldsymbol{c}_{12c} \cdot \boldsymbol{t})/(1/m_1 + r_1^2/I_1 + 1/m_2 + r_2^2/I_2). \tag{A 9}$$

Equations (A 7) and (A 9) are alternative frictional closure equations. The lesser of the tangential impulses is used with the normal impulse to calculate the components of the collisional impulse in the frame of reference of the general flow. The post-collision velocities are then calculated using (A 3) and (A 4*a*, *b*).

REFERENCES

BAGNOLD, R. A. 1954 Experiments on a gravity-free dispersion of large solid spheres in a Newtonian fluid under shear. *Proc. R. Soc. Lond.* A **225**, 49–63.

CAMPBELL, C. S. 1986 The effect of microstructure development on the collisional stress tensor in a granular flow. *Acta Mech.* **63**, 61–72.

CAMPBELL, C. S. 1989 The stress tensor for simple shear flows of a granular material. *J. Fluid Mech.* **203**, 449–473.

CARNAHAN, N. F. & STARLING, K. E. 1969 Equations of state for non-attracting rigid spheres. *Chem. Phys.* **51**, 635–636.

CHAPMAN, S. & COWLING, T. G. 1970 *The Mathematical Theory of Non-Uniform Gases*, 3rd ed. Cambridge University Press.

HOPKINS, M. A. 1987 Constitutive relations for rapidly sheared granular flows: a Monte Carlo form based on the kinetic theory of dense gases. PhD dissertation, Clarkson University, Potsdam, New York.

HOPKINS, M. A. & LOUGE, M. Y. 1991 Inelastic micro-structure in rapid granular flows of smooth disks. *Phys. Fluids* A **3** (1), 47–57.

JEANS, J. 1948 *An Introduction to the Kinetic Theory of Gases*. Cambridge University Press.

JENKINS, J. T. & RICHMAN, M. W. 1988 Plane simple shear of smooth, inelastic circular disks: the anisotropy of the fluctuation energy in the dilute and dense limits. *J. Fluid Mech.* **192**, 313–328.

JENKINS, J. T. & SAVAGE, S. B. 1983 A theory for the rapid flow of identical, smooth, nearly elastic, spherical particles. *J. Fluid Mech.* **130**, 187–202.

LUN, C. K. K., SAVAGE, S. B., JEFFREY, D. J. & CHEPURNIY, N. 1984 Kinetic theories for granular flow: inelastic particles in a couette flow and slightly inelastic particles in a general flow field. *J. Fluid Mech.* **140**, 223–256.

RICHMAN, M. W. & CHOU, C. S. 1992 Constitutive theory for homogeneous granular shear flows of highly inelastic spheres. *J. Rheol.* (submitted).

SAVAGE, S. B. & JEFFREY, D. J. 1981 The stress tensor in a granular flow at high shear rates. *J. Fluid Mech.* **110**, 255–272.

WALTON, O. R. 1983 Particle-dynamics calculations of shear flow. *Mechanics of Granular Materials – New Models and Constitutive Relations* (ed. J. T. Jenkins & M. Satake), pp. 327–338. Elsevier.

WALTON, O. R. & BRAUN, R. L. 1986 Stress calculations for assemblies of inelastic spheres in uniform flow. *Acta Mech.* **63**, 73–86.